PHYSICAL REVIEW B VOLUME 13, NUMBER 1 1 JANUARY 1976

Paramagnetic relaxation line shape in the Mössbauer spectroscopy of $1/2 \rightarrow 3/2$ transitions in axial symmetry*

B. D. Dunlap and G. K. Shenoy
Argonne National Laboratory, Argonne, Illinois 60439

L. Asch†
Technische Universität München, 8046 Garching bei München, Germany

(Received 28 August 1975)

Hirst's theory for the line shape of Mössbauer spectra in the presence of paramagnetic relaxation phenomena is applied to the case of $1/2 \rightarrow 3/2$ transitions. A detailed procedure for obtaining the lineshape is given for the case of axial symmetry, including off-diagonal terms in the hyperfine Hamiltonian. This is applicable for example, to the 14.4-keV transition in ^{57}Fe or the 66.7-keV transition in ^{171}Yb. The theory is used to analyze the data for ^{171}Yb in the cubic compound $Cs_2NaYbCl_6$. The hyperfine parameter $A = -38.7 \pm 2.0$ mm/sec and relaxation rate $W = 185 \pm 24$ MHz are in good agreement with previous measurements utilizing the resonance of ^{170}Yb in this material.

INTRODUCTION

The use of Mössbauer-effect spectroscopy for studying paramagnetic relaxation phenomena has been known for several years.[1] However, its application has been rather limited in most of that time due to an inadequate development of theoretical approaches for the problems of greatest interest. In most cases, detailed treatment has been limited to simple cases. For example, the situation when the electronic state is a highly anisotropic Kramer's doublet (the so-called effective-field case)[1,2] has been extensively used, even in cases where it did not apply, because of its inherent simplicity. However, only a few discussions exist for more complicated situations which include off-diagonal terms in the Hamiltonian.[3-7] The best known approaches are the stochastic method developed by Blume and coworkers,[3,4] and the perturbation approach which is put in the most useful form by Hirst.[6] Recently, Hirst's theory has been discussed and applied by Gonzalez-Jimenez *et al.* to give a closed-form expression for the resonance line shape in the presence of relaxation effects for $0 \rightarrow 2$ Mössbauer transitions, covering a relatively wide range of possible interactions.[7]

With regard to experimental work, the recent discovery of slow relaxation effects in the cubic compounds of the form Cs_2NaXCl_6 (X is a trivalent lanthanide ion) has provided one with a system where many of the relaxation phenomena for more complicated hyperfine interactions may be explored.[8,9] To present, these investigations have also been limited to $0 \rightarrow 2$ transitions for isotopes in the lanthanide series. In this paper we present Mössbauer-effect spectra taken at low temperatures for the compound $Cs_2NaYbCl_6$ using the 66.7-keV, $\frac{1}{2} \rightarrow \frac{3}{2}$ transition in ^{171}Yb. In considering the data obtained, we have worked out details of the relaxation line shape for $\frac{1}{2} \rightarrow \frac{3}{2}$ transitons in a case of axial symmetry using Hirst's approach.[6] In the following we discuss first the theoretical formalism for this case, and then apply those results to the data of $Cs_2Na\,^{171}YbCl_6$.

THEORY

In dealing with problems where the hyperfine interaction is very general, we must consider the way in which each possible transition is coupled to all others.[10] Thus we take as a basis vector, a four-index entity which specifies the nuclear ground-state spin, I_z^g, the electronic spin when the nucleus is in the ground state, S_z^g, and the corresponding spins in the excited state, I_z^e and S_z^e. Thus the basis vector is $|S_z^g, I_z^g, S_z^e, I_z^e\rangle \equiv |\mu n \nu m\rangle$. Considering all possible combinations, there are $(2I^g+1)(2I^e+1)(2S+1)^2$ such states and, for a very general hyperfine interaction, each of them corresponds to a possible transition. The relaxation process is then to be thought as a switching between these various states, i.e., a fluctuation among the possible transitions for the system of interest. The line shape of the Mössbauer spectrum $I(\omega)$ has been given by several authors,[6,7] and can be written in the following form:

$$I(\omega) = \mathrm{Re}[F(p)], \qquad (1)$$

where

$$F(p) = \sum_{\text{all indices}} \langle \mu n | M_{LM}^\dagger | \nu m \rangle \times \langle \mu n \nu m | \bar{U} | \mu' n' \nu' m' \rangle \times \langle \nu' m' | M_{LM} | \mu' n' \rangle \,. \qquad (2)$$

Here M_{LM} is an electromagnetic operator and $\overline{U}$ is an operator carrying all the essential physics, to be discussed below. Since in a Mössbauer experiment M_{LM} operates only on nuclear quantities, we have

$$\begin{aligned} \langle \nu' m' | M_{LM} | \mu' n' \rangle &= \delta_{\nu'\mu'} C^{LM}_{m'n'} , \\ \langle \mu n | M^{\dagger}_{LM} | \nu m \rangle &= \delta_{\mu\nu} (C^{LM}_{nm})^{\dagger} . \end{aligned} \tag{3}$$

The C^{LM}_{nm} are probability amplitudes for a transition from a nuclear state m to a state n with multipolarity L and polarization M. These are tabulated for powder samples in Table I for $I_g = \frac{1}{2} \rightarrow I_e = \frac{3}{2}$ transitions in both $M1$ (magnetic dipole, $L = 1$) and $E2$ (electric quadrupole, $L = 2$) cases.

Substituting Eq. (3) into Eq. (2) then gives for a given multipolarity L,

$$F(p) = \sum_{\text{all indices}} (C^{LM}_{nm})^{\dagger} C^{LM}_{m'n'} \langle \mu n \mu m | \overline{U} | \mu' n' \mu' m' \rangle . \tag{4}$$

The matrix elements of $\overline{U}$ in this equation can be shown to be related to the inverse of a matrix $\underline{U}$, discussed in the next paragraph, and Eq. (4) can conveniently be put into a matrix form

$$F(p) = \sum_{L,M} (\underline{C}^{LM})^{\dagger} \cdot \underline{U}^{-1} \cdot \underline{C}^{LM} . \tag{5}$$

Here it is understood from Eqs. (3) and (4) that the only contributions to the spectrum will come from those elements of $\underline{U}^{-1}$ which have $\mu = \nu$ and $\mu' = \nu'$.

The problem to be solved now consists of forming $\underline{U}$ and obtaining its inverse. This matrix can be written[6,7]

$$\underline{U} = p\underline{1} - (i/\hbar)\mathcal{H}^{+}_{0} - \underline{R} , \tag{6}$$

where $p = \Gamma - i\omega$, and Γ is the natural halfwidth of the resonance lines. $\mathcal{H}^{+}_{0}$ is a Liouville operator formed from the static (no relaxation effects) Hamiltonian $\mathcal{H}_0$ of the ion and has matrix elements[11]

$$\begin{aligned} \langle \mu n \nu m | \mathcal{H}^{+}_{0} | \mu' n' \nu' m' \rangle &= \delta_{\nu\nu'} \delta_{mm'} \langle \mu n | \mathcal{H}_0 | \mu' n' \rangle \\ &- \delta_{\mu\mu'} \delta_{nn'} \langle \nu' m' | \mathcal{H}_0 | \nu m \rangle . \end{aligned} \tag{7}$$

Here we consider a case of axial symmetry around the ion in question and take for $\mathcal{H}_0$ the hyperfine interaction. In the excited state this will be

$$\begin{aligned} \mathcal{H}_0 = \mathcal{H}_{\text{hf}} &= A^{*}_{\parallel} I^{e}_{z} S^{e}_{z} + \tfrac{1}{2} A^{*}_{\perp} (I^{e}_{+} S^{e}_{-} + I^{e}_{-} S^{e}_{+}) \\ &+ \beta [3 I^{e^2}_{z} - I^{e}(I^{e} + 1)] , \end{aligned} \tag{8}$$

where $A^{*}_{\parallel}$ and $A^{*}_{\perp}$ are the magnetic hyperfine constants and $\beta = e^2 q Q / 4 I^{e}(2 I^{e} - 1)$ is the quadrupole hyperfine constant. In the ground state, a similar equation applies with $A^{*}_{\parallel}$ and $A^{*}_{\perp}$ replaced by the ground-state parameters $A_{\parallel}$ and $A_{\perp}$, and with $\beta = 0$ for $I^{g} = \frac{1}{2}$.

TABLE I. Transition probability amplitudes C^{LM}_{nm} for nuclear spins $I^{g} = \frac{1}{2}$ and $I^{e} = \frac{3}{2}$ with $M1$ and $E2$ character.

n	m	M	$L = 1$	$L = 2$
$\frac{1}{2}$	$\frac{3}{2}$	1	$\sqrt{\frac{3}{12}}$	$\sqrt{\frac{1}{20}}$
$\frac{1}{2}$	$\frac{1}{2}$	0	$\sqrt{\frac{2}{12}}$	$\sqrt{\frac{2}{20}}$
$\frac{1}{2}$	$-\frac{1}{2}$	-1	$\sqrt{\frac{1}{12}}$	$\sqrt{\frac{3}{20}}$
$\frac{1}{2}$	$-\frac{3}{2}$	-2	0	$\sqrt{\frac{4}{20}}$
$-\frac{1}{2}$	$\frac{3}{2}$	2	0	$-\sqrt{\frac{4}{20}}$
$-\frac{1}{2}$	$\frac{1}{2}$	1	$\sqrt{\frac{1}{12}}$	$-\sqrt{\frac{3}{20}}$
$-\frac{1}{2}$	$-\frac{1}{2}$	0	$\sqrt{\frac{2}{12}}$	$-\sqrt{\frac{2}{20}}$
$-\frac{1}{2}$	$-\frac{3}{2}$	-1	$\sqrt{\frac{3}{12}}$	$-\sqrt{\frac{1}{20}}$

The matrix R in Eq. (6) carries all information concerning the relaxation processes prevalent. We assume that the pertinent interaction is adequately described as a coupling of the electronic moment with a fluctuating magnetic field $\overline{H}$,

$$\mathcal{H}_1 = g_{\parallel} \mu_B S_z \overline{H}_z + g_{\perp} \mu_B (S_x \overline{H}_x + S_y \overline{H}_y) . \tag{9}$$

We further assume that the time-averaged fluctuating field is the same in all directions. The relaxation matrix then depends only on a spectral density J involving a time averaged correlation function for the field $\overline{H}$, and results in two relaxation frequencies $W_{\parallel}$ and $W_{\perp}$ given by

$$W_{\parallel} = \tfrac{1}{2} g^{2}_{\parallel} J , \quad W_{\perp} = \tfrac{1}{2} g^{2}_{\perp} J . \tag{10}$$

In terms of these quantities, the relaxation matrix for $S = \frac{1}{2}$ becomes[7]

$$\begin{aligned} \langle \mu n \nu m | R | \mu' n' \nu' m' \rangle \\ = \delta_{nn'} \delta_{mm'} [\delta_{\mu\mu'} \delta_{\nu\nu'} (-\tfrac{1}{2} W_{\parallel} - W_{\perp}) \\ + 2 W_{\parallel} \langle \nu | S_z | \nu' \rangle \langle \mu' | S_z | \mu \rangle \\ + W_{\perp} (\langle \nu | S_{+} | \nu' \rangle \langle \mu' | S_{-} | \mu \rangle \\ + \langle \nu | S_{-} | \nu' \rangle \langle \mu' | S_{+} | \mu \rangle)] . \end{aligned} \tag{11}$$

For the case we wish to consider, we have $I^{g} = \frac{1}{2}$, $I^{e} = \frac{3}{2}$ and $S = \frac{1}{2}$. The dimensionality of the matrix $\underline{U}$ is thus 32. Inversion of this matrix point by point to form a spectrum as in Eq. (5) is a time consuming process even for large computers. Fortunately, the structure of the matrix is such that it can be factorized into small matrices, as was previously shown for the case of $0 \rightarrow 2$ transitions.[7] Considering Eqs. (7) and (8), one sees that the only nondiagonal states coupled by $\mathcal{H}^{+}_{0}$ are those for which $\mu + n = \mu' + n'$ or $\nu + m = \nu' + m'$. Similarly, from Eq. (11) we see for $S = \frac{1}{2}$ that R only couples states for which $\mu = \nu$, $\mu' = \nu'$, $m = m'$, and $n = n'$. By inspection of the 32 possible states in light of these requirements, it is found that the full matrix $\underline{U}$ can be divided into seven independent submatrices having dimensionalities N=1, 1, 4, 4, 7, 7, and 8. The first of these arises from the basis state $|-\frac{1}{2}, -\frac{1}{2}, +\frac{1}{2}, +\frac{3}{2}\rangle$ and the second from the state in which these spin projections all have the opposite sign. Neither of these will contribute to the spectrum because of the requirement of Eq. (4) that $\mu = \nu$. The two $N = 4$ matrices are found to be identical as are the two N= 7 matrices. Thus calculation of the spectrum requires handling of three matrices having $N = 4, 7, 8$. In the following we denote these by $\underline{a}$, $\underline{b}$ and $\underline{d}$ respectively.

The basis vectors for one of the $N = 4$ matrices are given in Table II. The basis vectors for the other is obtained by reversing all signs in Table II. Both sets, as stated above, give the same matrix $\underline{a}$, which can be calculated straightforwardly by application of Eqs. (6), (7), (8), and (11). The nonvanishing matrix elements a_{ij} are tabulated in Table III. From Table II, one sees that the requirement $\mu = \nu$ is satisfied only for the second and fourth basis states. Thus, one needs to calculate only the inverse elements a_{22}^{-1}, a_{44}^{-1}, a_{24}^{-1}, and a_{42}^{-1}, and the last two are equal. For this case the inverse can be worked out in closed form, and Eq. (5) yields

$$F_a(p) = |C^{L2}_{-1/2,3/2}|^2 (N_{22} + N_{44} + 2N_{24})/D, \qquad (12)$$

where

$$\begin{aligned} N_{22} &= a_{11}(a_{33}a_{44} - a_{34}^2), \\ N_{44} &= a_{33}(a_{11}a_{22} - a_{12}^2), \\ N_{24} &= -a_{11}a_{24}a_{33}, \qquad (13) \\ D &= a_{11}(a_{22}a_{33}a_{44} - a_{24}^2a_{33} - a_{34}^2a_{22}) \\ &\quad - a_{12}^2(a_{33}a_{44} - a_{34}^2). \end{aligned}$$

The $N = 7$ and $N = 8$ matrices are too cumbersome to allow a simple closed form expression, and their inversion must be done numerically. The basis states for the $N = 7$ matrix are given in Table IV and the matrix elements b_{ij} appear in Table V.

TABLE II. Basis vectors for one of the $N = 4$ matrices. The other set of vectors is obtained by changing all signs in the table.

State	μ	n	ν	m
1	$-\frac{1}{2}$	$-\frac{1}{2}$	$\frac{1}{2}$	$\frac{1}{2}$
2	$-\frac{1}{2}$	$-\frac{1}{2}$	$-\frac{1}{2}$	$\frac{3}{2}$
3	$-\frac{1}{2}$	$\frac{1}{2}$	$\frac{1}{2}$	$\frac{3}{2}$
4	$\frac{1}{2}$	$-\frac{1}{2}$	$\frac{1}{2}$	$\frac{3}{2}$

TABLE III. Matrix elements a_{ij} for the $N = 4$ matrix. Elements are also obtained by transposing $a_{ji} = a_{ij}$. All others vanish.

i	j	a_{ij}
1	1	$p + W_{\parallel} + W_{\perp} - i[\frac{1}{4}(A_{\parallel} - A_{\parallel}^*) + \beta]$
1	2	$\frac{1}{2}i\sqrt{3}A_{\perp}^*$
2	2	$p + W_{\perp} - i[\frac{1}{4}(A_{\parallel} + 3A_{\parallel}^*) - \beta]$
2	4	$-W_{\perp}$
3	3	$p + W_{\parallel} + W_{\perp} + i[\frac{1}{4}(A_{\parallel} + 3A_{\parallel}^*) + \beta]$
3	4	$-\frac{1}{2}iA_{\perp}$
4	4	$p + W_{\perp} + i[\frac{1}{4}(A_{\parallel} + 3A_{\parallel}^*) + \beta]$

Equations (4) and (5) then yield

$$\begin{aligned} F_b(p) = {} & |C^{L1}_{1/2,3/2}|^2(b_{11}^{-1} + b_{22}^{-1} + 2b_{12}^{-1}) \\ & + |C^{L1}_{-1/2,1/2}|^2(b_{44}^{-1} + b_{66}^{-1} + 2b_{46}^{-1}) \\ & + 2C^{L1}_{1/2,3/2}C^{L1}_{-1/2,1/2}(b_{14}^{-1} + b_{16}^{-1} + b_{24}^{-1} + b_{26}^{-1}). \end{aligned} \qquad (14)$$

Similarly, for the $N = 8$ matrix, the basis vectors and matrix elements d_{ij} are given in Table VI and VII, and one obtains

$$\begin{aligned} F_d(p) = {} & |C^{L0}_{1/2,1/2}|^2(d_{22}^{-1} + d_{33}^{-1} + 2d_{23}^{-1}) \\ & + |C^{L0}_{-1/2,-1/2}|^2(d_{55}^{-1} + d_{77}^{-1} + 2d_{57}^{-1}) \\ & + 2C^{L0}_{1/2,1/2}C^{L0}_{-1/2,-1/2}(d_{25}^{-1} + d_{27}^{-1} + d_{35}^{-1} + d_{37}^{-1}). \end{aligned} \qquad (15)$$

Calculation of the line shape for a given multipolarity L is then obtained from

$$I(\omega) = \mathrm{Re}[2F_a(p) + 2F_b(p) + F_d(p)]. \qquad (16)$$

It may be noted that the factorization discussed above is only possible for a restricted $\mathcal{H}_0$. One may add an external field parallel to the z axis as

TABLE IV. Basis vectors for one of the $N = 7$ matrices. The other set of vectors is obtained by changing all signs in the table.

State	μ	n	ν	m
1	$\frac{1}{2}$	$\frac{1}{2}$	$\frac{1}{2}$	$\frac{3}{2}$
2	$-\frac{1}{2}$	$\frac{1}{2}$	$-\frac{1}{2}$	$\frac{3}{2}$
3	$\frac{1}{2}$	$-\frac{1}{2}$	$-\frac{1}{2}$	$\frac{3}{2}$
4	$\frac{1}{2}$	$-\frac{1}{2}$	$\frac{1}{2}$	$\frac{1}{2}$
5	$-\frac{1}{2}$	$\frac{1}{2}$	$\frac{1}{2}$	$\frac{1}{2}$
6	$-\frac{1}{2}$	$-\frac{1}{2}$	$-\frac{1}{2}$	$\frac{1}{2}$
7	$-\frac{1}{2}$	$-\frac{1}{2}$	$\frac{1}{2}$	$-\frac{1}{2}$

TABLE V. Matrix elements b_{ij} for the $N=7$ matrix. Elements are also obtained by transposing $b_{ji}=b_{ij}$. All others vanish.

i	j	b_{ij}
1	1	$p+W_\perp-i[\frac{1}{4}(A_\parallel-3A_\parallel^*)-\beta]$
1	2	$-W_\perp$
2	2	$p+W_\perp+i[\frac{1}{4}(A_\parallel-3A_\parallel^*)+\beta]$
2	3	$-\frac{1}{2}iA_\perp$
2	5	$\frac{1}{2}i\sqrt{3}A_\perp^*$
3	3	$p+W_\parallel+W_\perp+i[\frac{1}{4}(A_\parallel-3A_\parallel^*)+\beta]$
3	4	$\frac{1}{2}i\sqrt{3}A_\perp^*$
4	4	$p+W_\perp+i[\frac{1}{4}(A_\parallel+A_\parallel^*)-\beta]$
4	5	$-\frac{1}{2}iA_\perp$
4	6	$-W_\perp$
5	5	$p+W_\parallel+W_\perp+i[\frac{1}{4}(A_\parallel+A_\parallel^*)-\beta]$
6	6	$p+W_\perp-i[\frac{1}{4}(A_\parallel+A_\parallel^*)+\beta]$
6	7	$iA_\perp^*$
7	7	$p+W_\parallel+W_\perp-i[\frac{1}{4}(A_\parallel+A_\parallel^*)+\beta]$

a straightforward generalization of the above. However, introduction of a nonaxial hyperfine interaction ($A_x\neq A_y\neq A_z\neq 0$), a nonaxial quadrupole interaction ($\eta\neq 0$), an external field at an arbitrary direction to the z axis, or incommensurate magnetic and quadrupole principal axes will destroy the factorization, and cause the necessity of treating the entire 32×32 matrix as an undivided unit. In such cases, procedures are available which substantially reduce the required computational time.[12] Some cases of this kind will be discussed by us in future publications. It may be noted that calculation of a 200 point spectrum using the subdivided matrix described here has taken approximately three seconds on an IBM 370/195 computer. Least-square fitting of data is therefore a very feasible procedure.

TABLE VI. Basis vectors for the $N=8$ matrix.

State	μ	n	ν	m
1	$\frac{1}{2}$	$\frac{1}{2}$	$-\frac{1}{2}$	$\frac{3}{2}$
2	$\frac{1}{2}$	$\frac{1}{2}$	$\frac{1}{2}$	$\frac{1}{2}$
3	$-\frac{1}{2}$	$\frac{1}{2}$	$-\frac{1}{2}$	$\frac{1}{2}$
4	$\frac{1}{2}$	$-\frac{1}{2}$	$-\frac{1}{2}$	$\frac{1}{2}$
5	$\frac{1}{2}$	$-\frac{1}{2}$	$\frac{1}{2}$	$-\frac{1}{2}$
6	$-\frac{1}{2}$	$\frac{1}{2}$	$\frac{1}{2}$	$-\frac{1}{2}$
7	$-\frac{1}{2}$	$-\frac{1}{2}$	$-\frac{1}{2}$	$-\frac{1}{2}$
8	$-\frac{1}{2}$	$-\frac{1}{2}$	$\frac{1}{2}$	$-\frac{3}{2}$

TABLE VII. Matrix elements d_{ij} for the $N=8$ matrix. Elements are also obtained by transposing $d_{ji}=d_{ij}$. All others vanish.

i	j	d_{ij}
1	1	$p+W_\parallel+W_\perp-i[\frac{1}{4}(A_\parallel+3A_\parallel^*)-\beta]$
1	2	$\frac{1}{2}i\sqrt{3}A_\perp^*$
2	2	$p+W_\perp-i[\frac{1}{4}(A_\parallel-A_\parallel^*)+\beta]$
2	3	$-W_\perp$
3	3	$p+W_\perp+i[\frac{1}{4}(A_\parallel-A_\parallel^*)-\beta]$
3	4	$-\frac{1}{2}iA_\perp$
3	6	$iA_\perp^*$
4	4	$p+W_\parallel+W_\perp+i[\frac{1}{4}(A_\parallel-A_\parallel^*)-\beta]$
4	5	$iA_\perp^*$
5	5	$p+W_\perp+i[\frac{1}{4}(A_\parallel-A_\parallel^*)-\beta]$
5	6	$-\frac{1}{2}iA_\perp$
5	7	$-W_\perp$
6	6	$p+W_\parallel+W_\perp+i[\frac{1}{4}(A_\parallel-A_\parallel^*)-\beta]$
7	7	$p+W_\perp-i[\frac{1}{4}(A_\parallel-A_\parallel^*)+\beta]$
7	8	$\frac{1}{2}i\sqrt{3}A_\perp^*$
8	8	$p+W_\parallel+W_\perp-i[\frac{1}{4}(A_\parallel+3A_\parallel^*)-\beta]$

APPLICATION TO $Cs_2Na^{171}YbCl_6$

We wish now to consider the case of the cubic compound $Cs_2NaYbCl_6$. The crystal-field ground state is well established from our previous work using ^{170}Yb Mössbauer spectroscopy to be a Γ_6 Kramers doublet.[8] Analysis of the magnetic susceptibility of this compound shows that the first excited state (Γ_8) is about 400 K above the ground state.[13] Thus at liquid-helium temperatures one has a well-isolated electronic configuration with cubic symmetry. In the above we therefore take $A_\parallel^*=A_\perp^*\equiv A^*$, $A_\parallel=A_\perp\equiv A$, $W_\parallel=W_\perp\equiv W$, and $\beta=0$. In addition we note that for this case an effective spin $S=\frac{1}{2}$ is appropriate. The nuclear transition for ^{171}Yb is of mixed multipolarity, having a substantial $E2$ admixture to the more common $M1$ transition. Previous work[14] has shown the mixing ratio to be $\delta^2=E2/M1=0.36$. In our calculations we have obtained the spectra by straightforwardly adding a theoretical line shape given by Eq. (16) for $L=2$ to that for $L=1$ with this relative intensity. Possible interference effects between dipole and quadrupole radiation will not be seen here, since such terms average to zero for powder samples.[15]

Spectra calculated using the values $A=-39.5$ mm/sec and $A^*/A=0.2361$, appropriate to ^{171}Yb in a Γ_6 state, are shown as a function of the re-

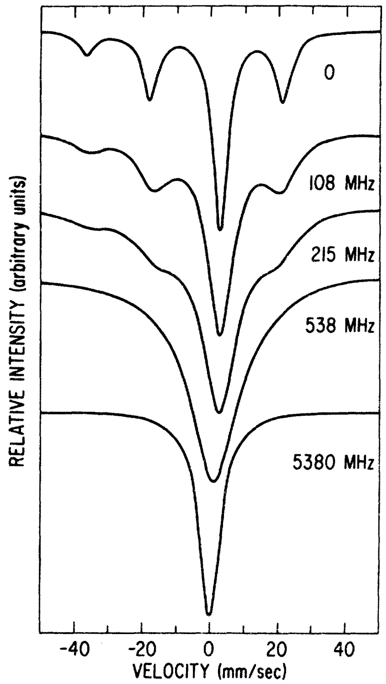

FIG. 1. Calculated Mössbauer-effect spectra for the 66.7-keV resonance of ^{171}Yb in a cubic crystal field having a Γ_6 electronic ground state. The hyperfine parameter is taken to be $A=-39.5$ mm/sec and the relaxation rate W varies as shown in the figure.

laxation frequency W in Fig. 1. The spectrum for $W=0$ is easily understood in light of previous discussions.[16] For both ground and excited states we define a total angular momentum $F=\vec{I}+\vec{S}$. Since $|S|=\frac{1}{2}$, we have $F^g=0, 1$ for the ground state and $F^e=1, 2$ for the excited state. The cubic hyperfine interaction $A\vec{I}\cdot\vec{S}$ then results in hyperfine energies given by

$$E_{\mathrm{hf}}=\tfrac{1}{2}A[F(F+1)-I(I+1)-S(S+1)] \qquad (17)$$

for the various F values (see Fig. 2). Transitions occur with the selection rules $\Delta F=0$, ± 1 for the $M1$ case and $\Delta F=0, \pm 1, \pm 2$, for the $E2$ case. Line positions and intensities for both are given in Table VIII, along with the intensities for the mixed multipolarity corresponding to ^{171}Yb. In Fig. 2 these transitions and their intensities are shown.

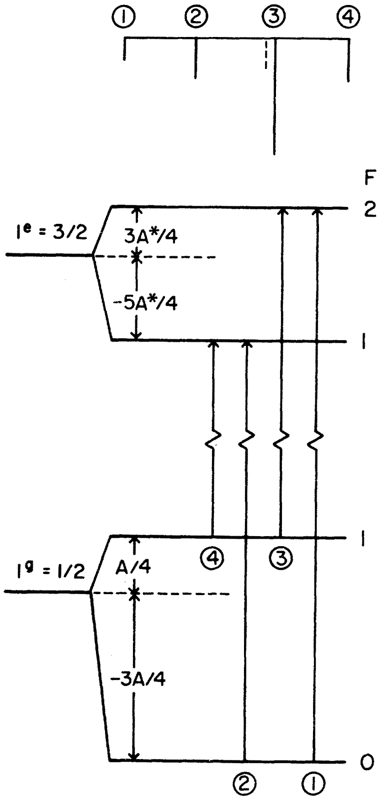

FIG. 2. Hyperfine energy-level scheme for $S=\frac{1}{2}$ case in cubic symmetry. The positions and relative intensities of various transitions in ^{171}Yb is shown by a bar diagram.

Figure 3 shows data obtained at 4.2 K using the 66.7 keV transition in ^{171}Yb for a $Cs_2NaYbCl_2$ absorber. The source material was ^{171}Tm in $ErAl_3$, prepared in the manner previously described.[14] The absorber was 110 mg/cm^2 total material of $Cs_2NaYbCl_6$, enriched to 88% in ^{171}Yb. The γ rays were detected with a 625-mm^2-area 5-mm-thick Ge(Li) solid state counter. A very low count rate (140 counts/sec in the single channel analyzer) was present, but data was collected for 8 days. Due to the high enrichment, the total effective intensity is almost 10%. The solid line shows the results of a least-squares fit using the formalism

TABLE VIII. Line positions and intensities for $\frac{1}{2}\to\frac{3}{2}$ transitions in cubic symmetry.

Transition	Position	F^g	F^e	Intensity $M1$	$E2$	$M1+0.36E2$
1	$\frac{3}{4}(A^*+A)$	0	2	0	$\frac{2}{8}$	0.090
2	$\frac{1}{4}(-5A^*+3A)$	0	1	$\frac{2}{8}$	0	0.250
3	$\frac{1}{4}(3A^*-A)$	1	2	$\frac{5}{8}$	$\frac{3}{8}$	0.760
4	$-\frac{1}{4}(5A^*+A)$	1	1	$\frac{1}{8}$	$\frac{3}{8}$	0.260

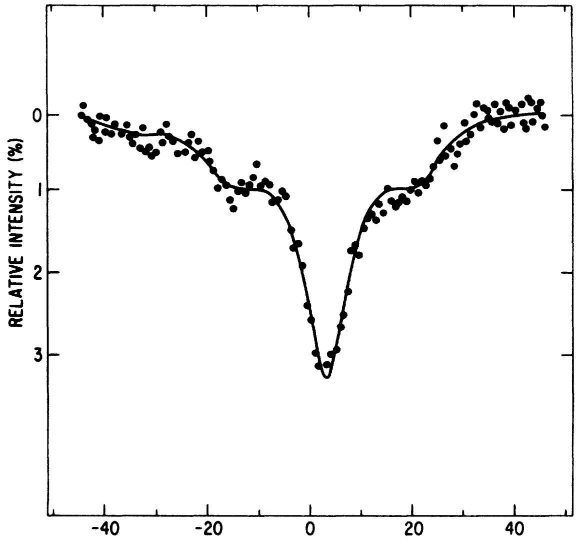

FIG. 3. Mössbauer effect spectrum for ^{171}Yb in $Cs_2NaYbCl_6$. The solid line is a least-squares fit obtained as described in the text.

discussed above. Good agreement with the detailed line shape is seen. In the fit, the linewidth (full width at half-maximum) has been fixed at 5.6 mm/sec, obtained with our source and single line absorbers. The relaxation frequency obtained is $W = 185 \pm 24$ MHz, compared with our previous value 206 ± 12 MHz obtained from the ^{170}Yb resonance in this material.[8] The A value obtained here is $^{171}A(\Gamma_6) = -38.7 \pm 2.0$ mm/sec $= (8.6 \pm 0.4) \times 10^{-6}$ eV. Converting this to an equivalent A value for the ^{170}Yb resonance using the known spins and nuclear moments gives $^{170}A(\Gamma_6) = (-2.92 \pm 0.17) \times 10^{-6}$ eV. This compares favorably with our previous measurement of $(-3.06 \pm 0.03) \times 10^{-6}$ eV using the ^{170}Yb Mössbauer effect in this compound.[8]

CONCLUSION

We have discussed paramagnetic hyperfine spectra and line-shape calculations in the presence of paramagnetic relaxation effects for the important case of $\frac{1}{2} - \frac{3}{2}$ transitions in Mössbauer-effect spectroscopy. Details have been given for calculating spectra via Hirst's theory for problems involving axial symmetry. The theory has been applied to measurements using the 66.7 keV resonance of ^{171}Yb in the compound $Cs_2NaYbCl_6$ to give hyperfine parameter and relaxation time at 4.2 K in agreement with previous values. Finally, we emphasize that the expressions developed here are directly applicable to a number of cases involving ^{57}Fe.

---

*Based on work performed in part under the auspices of the U. S. Energy Research and Development Administration.

†Stipendiatin der Alexander von Humboldt Stiftung, Germany; on leave from Laboratoire de Chimie Nucléaire, Strasbourg, France.

[1] H. H. Wickman, in *Mossbauer Effect Methodology*, edited by I. Gruverman (Plenum, New York, 1966), Vol 2, p. 39.

[2] H. H. Wickman, M. P. Klein, and D. A. Shirley, J. Chem. Phys. 42, 2113 (1965).

[3] M. Blume and J. A. Tjon, Phys. Rev. 165, 446 (1968).

[4] S. Dattagupta and M. Blume, Phys. Rev. B 10, 4540 (1974).

[5] H. H. Wickman and C. F. Wagner, J. Chem. Phys. 51, 435 (1969).

[6] L. L. Hirst, J. Phys. Chem. Solids 31, 655 (1970).

[7] F. Gonzalez-Jimenez, P. Imbert, and F. Hartmann-Boutron, Phys. Rev. B 9, 45 (1974).

[8] G. K. Shenoy, R. Poinsot, L. Asch, J. M. Friedt, and B. D. Dunlap, Phys. Lett. A 49, 429 (1974).

[9] G. K. Shenoy, L. Asch, J. M. Friedt, and B. D. Dunlap, J. Phys. (Paris) 35, C6-426 (1974).

[10] Much of the development and notation in this section parallels that of Ref. 7.

[11] M. Blume, Phys. Rev. 174, 351 (1968).

[12] G. K. Shevoy and B. D. Dunlap, Phys. Rev. B (to be published).

[13] B. D. Dunlap and G. K. Shenoy, Phys. Rev. B 12, 2716 (1975).

[14] W. Henning, G. M. Kalvius, and G. K. Shenoy, Phys. Rev. C 2, 2414 (1970).

[15] J. T. Dehn, J. G. Marzolf, and J. F. Salmon, Phys. Rev. 135, B1307 (1964).

[16] For example, see C. E. Johnson, J. Appl. Phys. 42, 1325 (1971).